2023 IEEE/ASME International Conference on Advanced Intelligent Mechatronics (AIM)
June 28-30, 2023. Seattle, Washington, USA

Optimal Multisine Perturbations for Improved Dynamic System Identification using a Mechanical Platform: A Preliminary Simulation Study

Yingxin Qiu[1], Mengnan Wu[2], Lena H. Ting[3], and Jun Ueda[1]

***Abstract*— This paper investigates the design of optimal inputs for dynamic system identification. Specifically, this paper concerns the perturbation design for system identification experiments where target human systems are perturbed by mechanical inputs produced by an active device. Although conventional perturbation design criteria are generally applicable, including the scenario described above, problems arise due to the dynamics of the active device. A low-bandwidth active device may distort the input signal and thereby void the optimality of the input. To address this issue, the paper formulates an optimization problem for optimal input design that explicitly incorporates the active device dynamics. The cost function is the determinant of a modified covariance lower bound that takes the active device dynamics into consideration. The proposed method is demonstrated with an identification of a linear dynamics model simulating human arm impedance. Simulation results show that, compared with a standard optimal input and an input with a flat spectrum, the proposed optimal input with active device compensation achieved a smaller parameter covariance. Furthermore, the proposed optimization problem suggests that the optimal covariance lower bound can be achieved by active devices with different dynamics properties. This allows the control design of the active device to satisfy a wide variety of requirements without sacrificing its ability to perform system identification.**

I. Introduction

Estimation of parametric models from experimental data is a common practice in science and engineering. While the selection of model structures and estimation algorithms are crucial, experimental design also plays an important role in determining the estimation accuracy. A mathematical approach to optimal experimental design for static models was surveyed in [1]. The technique was then extended to system identification of dynamic systems [2]–[5]. Recent works have been focusing on describing the input design problem as a convex optimization problem with modified cost functions and added constraints [6], [7]. By doing so, non-standard cost functions and constraints with practical considerations can be incorporated into the optimal experimental design problem, which can be solved efficiently using standard toolboxes and optimization solvers [8], [9].

The concept of optimal experimental design is to achieve the best estimation accuracy given a prescribed amount of resources. For dynamic system identification, a limitation on experimental resources may come from an allowable downtime of a process plant, or the maximum excitation levels of an active device. In human system identification, both the duration and excitation level must be carefully considered. In this context, the optimal experimental design seeks for power-limited input signals to perturb the target dynamic system such that the resulting parameter covariance is minimized. This is based on the fact that, when an unbiased estimator is used, the covariance matrix is lower bounded by the inverse of the Fisher information matrix [10]. Since the Fisher information matrix is a function of the input signal, it is possible to design inputs that maximize the Fisher information matrix to achieve the smallest covariance.

Designing optimal input signals requires some prior knowledge about the target system. That is to say, the optimality of the designed input is with respect to the current knowledge of the system. If such information is not available, the parameter estimation can be performed in an iterative process [6]. It is recommended to use an input signal with a flat spectrum to obtain an initial model. Then, based on this initial guess, an optimal input can be designed. The subsequent optimal inputs can be obtained by repeating the same process until a certain confidence level is reached. The nature of the optimal input design makes it suitable for identifying subtle changes in the target system, such as the changes in the robot dynamics caused by operations in the field, or changes in the human sensorimotor system due to intervention. This paper focuses on the design of optimal inputs for linear dynamic systems and the associated physical realization problem.

II. Problem Statement

Modeling of the human sensorimotor system can benefit from optimal input design given its success in identifying dynamic systems in other settings [11]–[13]. While the methodology of designing optimal inputs is generally applicable to any dynamic system, expected performances may not be always achieved in human system identification due to the involvement of active devices for physical input realization [14]. Typically, an active device used in human

This work was supported by National Science Foundation under Grant Nos. CMMI-M3X 1761679 and 1762211.

[1]Yingxin Qiu and Jun Ueda are with the George W. Woodruff School of Mechanical Engineering, Georgia Institute of Technology, Atlanta, GA 30332-0405, USA. (e-mail: yqiu47@gatech.edu; jun.ueda@me.gatech.edu)

[2]Mengnan Wu is with the W. H. Coulter Department of Biomedical Engineering, Emory University and Georgia Institute of Technology, Atlanta, GA 30332-4250, USA. (e-mail: mengnan.wu@emory.edu)

[3]Lena H. Ting is with the W. H. Coulter Department of Biomedical Engineering, Emory University and Georgia Institute of Technology, and Department of Rehabilitation Medicine, Division of Physical Therapy, Emory University, Atlanta, GA 30332-4250, USA. (e-mail: lting@emory.edu)

978-1-6654-7633-1/23/$31.00 ©2023 IEEE

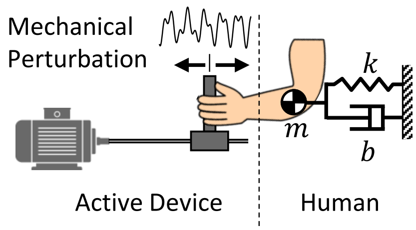

Fig. 1. Identification of human joint dynamics using a mechanical platform. A random mechanical input is applied to perturb the human system.

experiments is a manipulandum on the scale of human musculoskeletal systems. For example, Fig. 1 illustrates an experiment where a human arm is perturbed by a mechanical perturbation in order to estimate the arm impedance. Such devices often have limited bandwidths and act as a low-pass filter on optimally designed perturbations. Since the optimal inputs are designed based on either the correlation function or spectrum, this filtering effect degrades the input quality, leading to worse-than-expected performance.

In order to achieve the expected system identification performance, the physical realization of the optimal input must take into consideration of the active device dynamics. The authors have previously studied the physical realization of flat-spectrum perturbations [14], which is recommended to identify fully unknown target systems. Once an initial guess of the target system is obtained, the optimal input design can be performed. Similar to flat spectrum inputs, producing the optimal input using an actuated mechanical system is subject to degraded quality. This paper addresses the physical realization of the optimal input by incorporating device dynamics into the optimization problem formulation.

The standard optimal input in the frequency domain is the solution of a convex optimization problem that maximizes the Fisher information matrix. To handle the active device dynamics, a modified version of the Fisher information matrix is proposed as the new cost function of the optimization problem. The resulting optimal inputs already have the device dynamics compensated so that accurate system identification can be achieved.

III. METHODS

A. Fisher Information matrix of a linear SISO system

The proposed optimal input design improves the parameter estimation accuracy by optimally redistributing the power of the input signal that maximizes the Fisher information matrix. For a family of polynomial model structures, the information matrix that describes the amount of information captured by an input signal can be derived.

Consider a polynomial model structure in the form

$$\begin{aligned} y(t) &= G_1(s)x(t-\tau) + G_2(s)e(t) \\ &= \frac{B(s)}{A(s)}x(t-\tau) + \frac{D(s)}{C(s)}e(t) \end{aligned} \tag{1}$$

where $x(t)$ and $y(t)$ are the system input and output, $e(t)$ is the Gaussian white noise with unit variance, and τ is a known input delay. Suppose that the plant model and the error model are independently parameterized, $G_1(s)$ and $G_2(s)$ can be defined by

$$A(s) = 1 + a_1 s + ... + a_n s^n \tag{2}$$

$$B(s) = b_0 + b_1 s + ... + b_m s^m \tag{3}$$

$$C(s) = 1 + c_1 s + ... + c_q s^q \tag{4}$$

$$D(s) = d_0 + d_1 s + ... + d_r s^r \tag{5}$$

with $m \leq n$ and $r \leq q$. The unknown model parameters is denoted by

$$\theta = [a_1, ..., a_n, b_0, ...b_m, c_1, ...c_q, d_0, ...d_r]^T \in \Re^p \tag{6}$$

where $p = n+m+q+r+2$. If the output noise is Gaussian, the model reduces to

$$y(t) = \frac{B(s)}{A(s)}x(t-\tau) + d_0 e(t) \tag{7}$$

and the number of unknown parameters becomes $p = n + m + 1$.

The Fisher information matrix per unit time of (1) is given by [2]

$$\begin{aligned} \bar{M}_\theta = \frac{1}{2\pi}\int_{-\infty}^{\infty} \left[\frac{\partial G_1(j\omega)}{\partial\theta}\right] [G_2^{-1}(j\omega)][G_2^{-1}(j\omega)]^* \\ \left[\frac{\partial G_1(j\omega)}{\partial\theta}\right]^* \Phi_x(\omega)d\omega + \bar{M}_c \end{aligned} \tag{8}$$

where $\bar{M}_\theta$ is a p-by-p matrix, $\Phi_x(\omega)$ is the input spectrum, and the symbol $*$ denotes the complex conjugate transpose. It has been shown that $\bar{M}_c$ is not a function of the input, and therefore is a constant with respect to any input design [2]. The integral term in (8) can be simplified as

$$\bar{M} = \text{Re}\int_0^{\infty} h(j\omega)h^*(j\omega)\Phi_x(\omega)d\omega \tag{9}$$

where $h(s)$ is a p-vector with the i-th element

$$h_i(s) = \begin{cases} -e^{s\tau}\frac{CB}{DA^2}(s)s^i, & i = 1,..,n \\ e^{s\tau}\frac{C}{DA}(s)s^{(i-n-1)}, & i = 1+n,..,p \end{cases} \tag{10}$$

B. Convex optimization of the Information Matrix

According to the Cramer-Rao inequality, any unbiased estimator $\hat{\theta}$ of θ results in a covariance matrix that satisfies

$$cov\ \hat{\theta} \leq M_\theta^{-1}. \tag{11}$$

If a maximum likelihood estimator is used (or other asymptotically efficient estimators), M_θ^{-1} can be used as an approximation for $cov\ \hat{\theta}$ given long enough data [3]. From (9), the information matrix is determined by the input $\Phi_x(\omega)$. Therefore, the problem of improving the parameter estimation accuracy can be converted into the problem of designing $\Phi_x(\omega)$ such that $\bar{M}_\theta^{-1}$, or equivalently $\bar{M}^{-1}$, is small.

An optimal information matrix is traditionally quantified by the D-, A-, or E-optimality as

$$\text{D-optimal} \qquad \min -\log\det\bar{M} \tag{12}$$

$$\text{A-optimal} \qquad \min \text{trace}\bar{M}^{-1} \tag{13}$$

$$\text{E-optimal} \qquad \min \lambda_{\text{max}}\bar{M}^{-1} \tag{14}$$

The D-optimality is adopted here because the corresponding optimization problem is invariant to a nonsingular linear transformation of the model parameters. Also note that the D-optimal criteria as well as the other two are convex in input spectrum $\Phi_x(\omega)$, so an efficient optimization solver can be used for each of the optimality criteria.

By discretizing the input spectrum into a line spectrum with Q components,

$$\Phi_x(\omega) = \sum_{i=1}^{Q} \lambda_i \delta(\omega - \omega_i), \tag{15}$$

the standard power-constrained input optimization problem can be described as

$$\begin{aligned} \min_{\lambda_i}. \quad & -\log\det\left[\mathrm{Re}\sum_{i=1}^{Q}\lambda_i h(j\omega_i)h^*(j\omega_i)\right] \\ \text{s.t.} \quad & \sum_{i=1}^{Q}\lambda_i = 1 \\ & \lambda_i \geq 0. \end{aligned} \tag{16}$$

Selecting a small value for Q reduces the parameter space, however, to ensure that the information matrix is nonsingular, Q must be greater than or equal to p. The optimal cost corresponds to the smallest achievable $\bar{M}^{-1}$. A globally optimal solution is guaranteed because it is a convex optimization problem.

C. Input signal synthesis

The optimal input design returned by (16) specifies a power distribution in the frequency domain. To generate physical perturbations, time-domain realization of the optimal spectrum is required. A standard approach is to construct a multisine signal as

$$r(t) = \sum_{i=1}^{Q} \sqrt{2\lambda_i}\sin(\omega_i t + \phi_i). \tag{17}$$

The values of λ_i are determined by the input optimization, but ϕ_i remains to be determined. Using 0 phases at all frequencies will likely produce a signal with a large peak amplitude that is not desirable for many system identification experiments. Instead, Schroeder phase [15] defined as $\phi_i = -i(i-1)\pi/Q$ may be used. If ω_i's are harmonically related with ω_1 being the fundamental frequency, $r(t)$ is periodic and has a period of $(2\pi/\omega_1)$ s.

D. Optimal input design with dynamics compensation

The standard input design problem in (16) returns a power distribution $\Phi_x(\omega)$ which can be synthesized into a reference signal in the time domain using (17). In conventional system identification, this signal could be an electrical signal generated using an arbitrary waveform generator or a digital signal stored in a digital computer. In either case, $r(t)$ can be generated without significant distortions. On the other hand, when $r(t)$ is used as a reference to generate mechanical perturbations, the signal must go through a process shown in Fig. 2. The actual perturbation acting on the target system

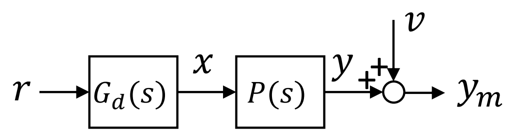

Fig. 2. System identification using a mechanical perturbation generated with an active device. r is the optimized input signal. x is the mechanical perturbation generated by an active device $G_d(s)$. $P(s)$ is the target system with response y when subject to mechanical perturbation x. The output measurement y_m has an additive noise v.

$P(s)$ is $x(t)$ which differs from $r(t)$ due to the device dynamics $G_d(s)$.

To compensate for the dynamics of the mechanical device used to generate the perturbation, the modified problem is proposed

$$\begin{aligned} \min_{\lambda_i'}. \quad & -\log\det\left[\mathrm{Re}\sum_{i=1}^{Q}\lambda_i'|G_d(j\omega_i)|^2 h(j\omega_i)h^*(j\omega_i)\right] \\ \text{s.t.} \quad & \sum_{i=1}^{Q}\lambda_i'|G_d(j\omega_i)|^2 = 1 \\ & \lambda_i' \geq 0. \end{aligned} \tag{18}$$

λ_i' specifies the power distribution of the optimal input that compensates for the device dynamics $G_d(s)$. For any mechanical device, $|G_d(j\omega)| > 0$ at all frequencies. The time-domain input signal can be realized similarly using (17).

E. Impedance parameter estimation

A frequency domain approach is adopted to estimate the transfer function of the target system $P(s)$

$$\min_{P(s)} \sum_{k=1}^{N_f} \left| P(\omega_k) - \frac{Y(\omega_k)}{X(\omega_k)} \right|^2 \tag{19}$$

where $X(\omega_k)$ and $Y(\omega_k)$ are the discrete Fourier transform of the input and output measurements.

IV. Results

A. Simulation setup

The performance of the proposed optimal input design is validated by simulation where a human arm impedance model is identified. It is well-known that under consistent conditions, the human arm behaves as a mass-spring-damper system $Z_{arm} = ms^2 + bs + k$ [16]. This ideal arm impedance model is an improper transfer function and its magnitude response goes to infinity. A more realistic representation is $Z_{arm} = \frac{(ms^2+bs+k)}{L(s)}$ with a monic low-pass filter $1/L(s)$ of order greater or equal to 2. In this simulation, $1/L(s) = 1/((1/\omega_n^2)s^2 + (2\zeta/\omega_n)s + 1)$ is used. Impedance parameters used in the simulation are $m = 2, b = 30, k = 400, \zeta = 0.8, \omega_n = 40$. The Bode diagram of the filtered arm impedance model is shown in Fig. 3. The m, b and k values are from [16] which are a reasonable approximation of a typical arm impedance. The dynamics of the active device

$G_d(s) = \frac{198s+528}{0.02252s^3+11.66s^2+396.3s+528}$ is based on the motion platform developed by the authors [14], [17].

The simulation follows the block diagram shown in Fig. 2. r is the input reference used to generate physical perturbation x with an active device $G_d(s)$. y is the response of the target system subject to x. Since the system output in Fig. 2 represents the interaction force in this scenario, its measurement via a force sensor is likely to be noisy. Thus, a Gaussian white noise v with a variance of 0.1 is added to the output measurement. On the other hand, the position measurement, which is the input to the human arm model, is typically acquired by an encoder that is not susceptible to random noise.

B. Comparison of input signals

The performance of three input signals (r in Fig. 2) were compared. They are

- r_{uc}: optimal input without device dynamics compensation designed with (16).
- r_{flat}: input with a flat spectrum that satisfy the power constraint in (16).
- r_c: optimal input with device dynamics compensation designed with (18).

The spectra of r_{uc}, r_{flat}, and r_c are defined over a discrete set of frequencies within the range of $[0.25, 30]$ rad/s with a 0.25 rad/s increment. Their time domain realizations shown in Fig. 4 are obtained with (17). The spectra of these three input signals are shown in Fig. 5. The flat-spectrum input is noticeable by its even power distribution. This spectrum can be interpreted as an equal effort to probe different modes of the target systems. In contrast, the optimal inputs have regions with high power concentration. In the case of arm impedance identification, power is optimally allocated to improve the estimation of stiffness (low frequency), damping (corner frequency), and inertia (high frequency). Notice that the spectra of the r_c and r_{uc} have different shapes. The compensation for the device dynamics is therefore more than a constant scaling.

C. Parameter Estimation

For each input, simulation and parameter estimation were performed 50 times. Each simulation of the system in Fig. 2 yields an input-output dataset comprised of the noise-free position input x and the noisy force output y_m. The arm impedance model was estimated by (19) using the input-output data. The transfer function estimation includes the estimation of the low-pass filter $L(s)$. Equivalent m, b, and k parameters are recovered by dividing the numerator coefficients by the constant term of the denominator. The values of mean and standard deviations of m, b, and k are listed in Table I. The covariance matrices of the three tested inputs are

TABLE I
ARM IMPEDANCE PARAMETER ESTIMATION.

	Uncompensated	Flat Spectrum	Compensated
m	2.0153	2.0108	2.0017
	(0.1328)	(0.1209)	(0.0679)
b	30.0471	29.9910	30.0101
	(1.0462)	(0.9691)	(0.4972)
k	398.4796	398.7332	398.8890
	(12.3618)	(9.5681)	(6.9748)

standard deviation are in parentheses

TABLE II
PARAMETER ESTIMATION COVARIANCE.

	Uncompensated	Flat Spectrum	Compensated
det cov	1.6891	0.5307	0.0311
Tr cov	153.9267	92.5027	48.9001
$\lambda_{max} cov$	152.8992	91.7281	48.6669

$$cov_{uc} = \begin{bmatrix} 0.0016 & -0.0051 & 0.3529 \\ -0.0051 & 0.2978 & -0.8139 \\ 0.3529 & -0.8139 & 148.7982 \end{bmatrix}$$
$$cov_{flat} = \begin{bmatrix} 0.0008 & -0.0020 & 0.1778 \\ -0.0020 & 0.1897 & -0.3494 \\ 0.1778 & -0.3494 & 80.4743 \end{bmatrix}$$
$$cov_{c} = \begin{bmatrix} 0.0003 & -0.0009 & 0.0894 \\ -0.0009 & 0.0593 & -0.1130 \\ 0.0894 & -0.1130 & 41.4333 \end{bmatrix}.$$

The determinant, trace, and maximum eigenvalue of the covariance matrices are summarized in Table II.

Since the transfer function estimator in (19) is unbiased, all three types of input signals yielded accurate mean values of m, b, and k. However, the standard deviations are significantly different. For each impedance parameter, the standard deviation using the proposed optimal input (compensated) is about half of that using the uncompensated input. The standard deviations obtained by the flat-spectrum input are somewhere in between.

The mean, standard deviation, and covariance of the parameter estimation can be visualized in Fig. 6-8. The distribution of the 50 parameter estimations is shown, and the ellipses represent the 95% confidence regions. When all three parameters are considered, the confidence region becomes an ellipsoid. The determinant, trace, and maximum eigenvalue of a covariance matrix correspond to the volume, sum of axes, and the major axis of the ellipsoid [1]. Thus, the size of the ellipses reflects the relative magnitude of the covariance listed in Table II. Overall, the optimal input with compensation yields the most accurate parameter estimation, followed by the flat-spectrum input and the uncompensated optimal inputs. Note that this observation is specific to the arm impedance model and device dynamics used in the simulation. If the frequency components that the target system is sensitive to are not attenuated significantly by the device dynamics, using the uncompensated input may yield better performance than using the flat-spectrum input.

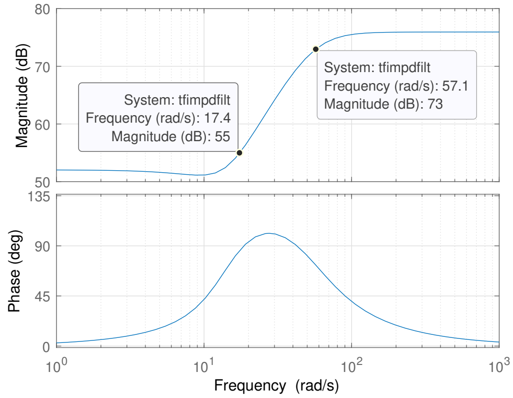

Fig. 3. Bode diagram of the arm impedance

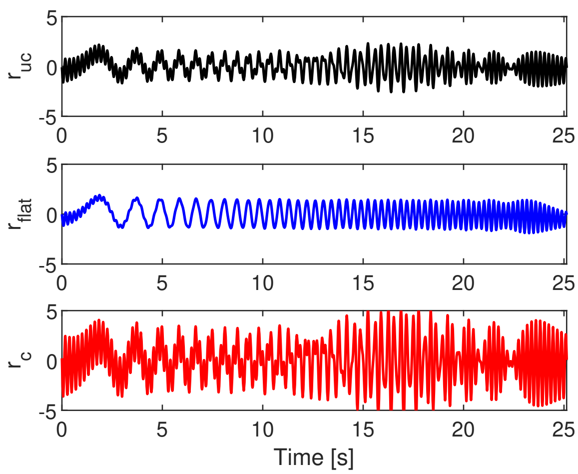

Fig. 4. Time-domain realization of input signals.

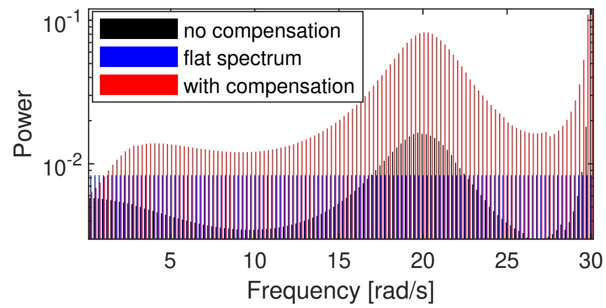

Fig. 5. Spectra of the input signals

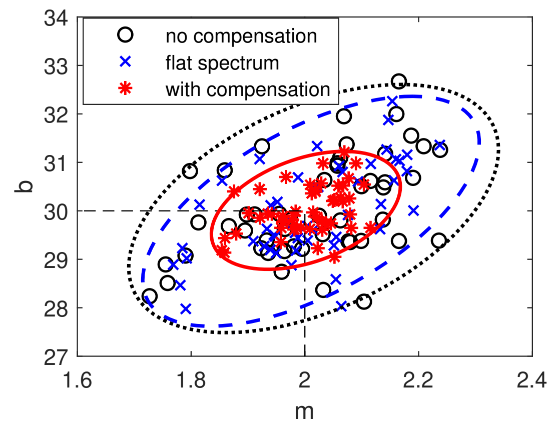

Fig. 6. Mass and damping parameter covariance.

V. Discussion

A. Active device dynamics

The optimization problem (18) computes an optimal input given the dynamics of a device. When the dynamics of a different device is provided, a different optimal input is generated. Theoretically, an optimal solution exists for any device dynamics that has a non-zero frequency response over the frequency range of interest. However, it is also important to investigate whether the same performance, quantified by the cost function of the optimization problem, can be achieved by different devices. The simulation results in Fig. 9 show that this is possible. Figure 9 presents the two combinations of device dynamics and input power distributions that achieved the same optimal information matrix. This result is significant because it suggests that optimal estimation accuracy may be achieved with different devices as long as the input signals are designed accordingly. Similarly, it also suggests that for a specific mechanical platform, the controller can be designed to satisfy additional requirements without sacrificing its capability of performing system identification. An example would be to implement a controller that prioritizes safe and natural physical human-robot interaction instead of achieving a high bandwidth.

B. Future works

Actuator command constraints: When an optimal input is designed to compensate for the device dynamics, the input magnitude may increase, especially when the device behaves as a low-pass filter. Larger input magnitudes will require larger actuator commands, which can potentially exceed the actuator capacity. To avoid excessive compensation, constraints on actuator command can be added to (18).

Robustness analysis: The optimal input design relies on prior knowledge of the target system. In practice, perfect knowledge is not available (system identification would not be needed otherwise); the improvement in estimation accuracy reported in Section IV may or may not be achieved. To understand how the estimation accuracy depends on prior knowledge, the robustness of the optimal input design with respect to uncertainty and variation in the model parameter should be analyzed.

Controller design for robustness improvement: The device dynamics included in the cost function of (18) has been treated as a source of performance degradation that needs to be compensated. However, it can also be considered as an extra degree of freedom, in addition to the input power distribution, to improve the optimal cost of (18) and therefore the estimation accuracy. Following the robustness analysis described above, one can use the frequency response of the

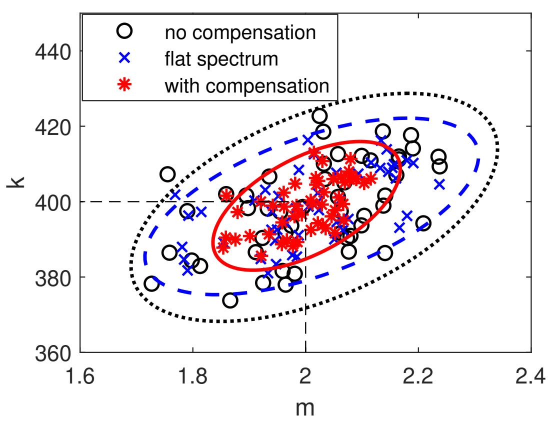

Fig. 7. Mass and stiffness parameter covariance

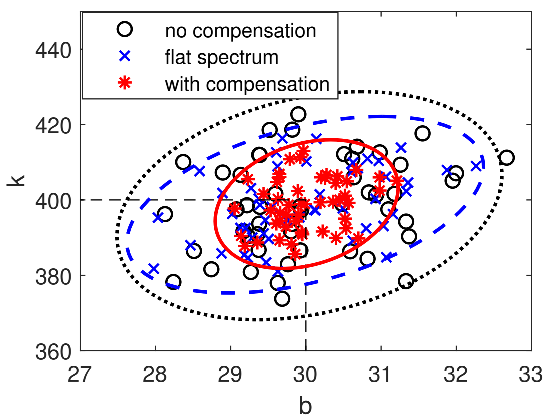

Fig. 8. Damping and stiffness parameter covariance

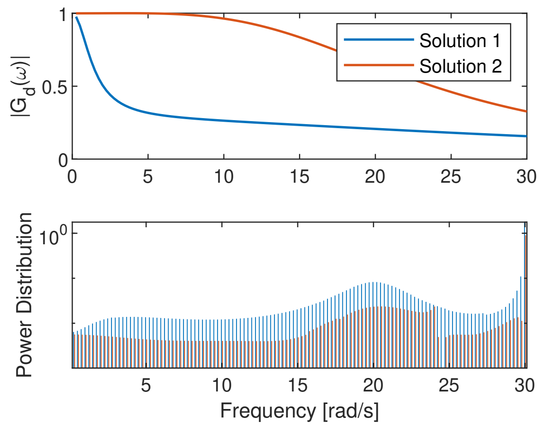

Fig. 9. Different combinations of device dynamics and input design that achieve the optimal information matrix

device as a weighting function to shape the sensitivity of the $h(j\omega_i)h^*(j\omega_i)$ term with respect to parameter uncertainty.

VI. Conclusion

This paper presented an optimal input design method for linear dynamic system identification using mechanical perturbations. The proposed method incorporated the dynamics of the active device in the design process so that the physical realization of the designed input will not cause degraded performance. The simulation showed that the proposed input design has improved estimation accuracy compared with the conventional optimal input and flat-spectrum input. In addition, the proposed input design formulation suggested that the same system identification performance can potentially be achieved by devices with different dynamics. This allows the active device to satisfy other control design requirements without sacrificing its capability of performing system identification.

References

[1] V. V. Fedorov, *Theory of optimal experiments*, ser. Probability and mathematical statistics: a series of monographs and textbooks. New York: Academic Press, 1972, no. 12.

[2] G. C. Goodwin and R. L. Payne, *Dynamic System Identification: Experiment Design and Data Analysis*, ser. Mathematics in Science and Engineering. New York: Academic Press, 1977, no. v 136.

[3] M. B. Zarrop, *Optimal Experiment Design for Dynamic System Identification*, ser. Lecture Notes in Control and Information Sciences. Berlin ; New York: Springer-Verlag, 1979, no. 21.

[4] R. Mehra, "Optimal input signals for parameter estimation in dynamic systems–Survey and new results," *IEEE Transactions on Automatic Control*, vol. 19, no. 6, pp. 753–768, Dec. 1974.

[5] R. K. Mehra, "Frequency-Domain Synthesis of Optimal Inputs for Linear System Parameter Estimation," *Journal of Dynamic Systems, Measurement, and Control*, vol. 98, no. 2, pp. 130–138, June 1976.

[6] M. Annergren, C. A. Larsson, H. Hjalmarsson, X. Bombois, and B. Wahlberg, "Application-Oriented Input Design in System Identification: Optimal Input Design for Control [Applications of Control]," *IEEE Control Systems Magazine*, vol. 37, no. 2, pp. 31–56, Apr. 2017.

[7] C. R. Rojas, J. S. Welsh, G. C. Goodwin, and A. Feuer, "Robust optimal experiment design for system identification," *Automatica*, vol. 43, no. 6, pp. 993–1008, June 2007.

[8] J. Löfberg, "Yalmip : A toolbox for modeling and optimization in matlab," in *In Proceedings of the CACSD Conference*, Taipei, Taiwan, 2004.

[9] S. P. Boyd, Ed., *Linear Matrix Inequalities in System and Control Theory*, ser. SIAM Studies in Applied Mathematics. Philadelphia: Society for Industrial and Applied Mathematics, 1994, no. vol. 15.

[10] L. Ljung, "System identification," *Wiley encyclopedia of electrical and electronics engineering*, pp. 1–19, 1999.

[11] R. Hildebrand and M. Gevers, "Identification For Control: Optimal Input Design With Respect To A Worst-Case ν-gap Cost Function," *SIAM Journal on Control and Optimization*, vol. 41, no. 5, pp. 1586–1608, Jan. 2002.

[12] S. Narasimhan and R. Rengaswamy, "Plant Friendly Input Design: Convex Relaxation and Quality," *IEEE Transactions on Automatic Control*, vol. 56, no. 6, pp. 1467–1472, June 2011.

[13] L. Pronzato, "Optimal experimental design and some related control problems," *Automatica*, vol. 44, no. 2, pp. 303–325, Feb. 2008.

[14] Y. Qiu, M. Wu, L. H. Ting, and J. Ueda, "Maximum Spectral Flatness Control of a Manipulandum for Human Motor System Identification," *IEEE Robotics and Automation Letters*, vol. 6, no. 2, pp. 3271–3278, Apr. 2021.

[15] M. Schroeder, "Synthesis of low-peak-factor signals and binary sequences with low autocorrelation (Corresp.)," *IEEE Transactions on Information Theory*, vol. 16, no. 1, pp. 85–89, Jan. 1970.

[16] A. C. Schouten, W. Mugge, and F. C. T. van der Helm, "NMClab, a model to assess the contributions of muscle visco-elasticity and afferent feedback to joint dynamics," *Journal of Biomechanics*, vol. 41, no. 8, pp. 1659–1667, Jan. 2008.

[17] M. Wu, Y. Qiu, J. Ueda, and L. H. Ting, "A Versatile Emulator for Haptic Communication to Alter Human Gait Parameters," *IEEE Robotics and Automation Letters*, vol. 7, no. 3, pp. 7335–7342, July 2022.